

Chapter 2

Frequency Analysis

2.1 Introduction

Jean Baptiste Joseph Fourier (1768–1830), a brilliant French mathematician, had the grace (or disgrace) to live at the time of Napoleon’s conquest of the civilized world. He joined Napoleon’s expedition to Egypt as scientific advisor, later becoming an Egyptologist and administrator for Napoleon’s government. It was during his time as prefect in Grenoble when he did his major work on heat conduction. It took him, however, nearly two decades to publish this work, mainly due to the proposal of a novel – and at the time controversial – way to decompose periodic signals into weighted sums of sine and cosine functions. This decomposition, in our days known as Fourier series, has been his major contribution to science, largely transcending its original application to heat conduction.

Following Fourier ideas, signals as the ones recorded from scalp EEG surface electrodes can be represented in the time domain or alternatively in terms of their decomposition into sines and cosines in the frequency domain. Take for example the oscillatory signal of Fig. 2.1a and suppose you want to transmit it to somebody else. You could in principle dictate all the time points of the sinusoid one by one, or alternatively you can just say that it is a sinusoid with a frequency of 10 Hz (i.e., a cycle repeating itself every 100 ms), as represented in the frequency plot of the lower left panel. These two views seem analogous, though you may also say that the frequency representation appears to be more compact and simple. Take now the example of Fig. 2.1b on the right hand side. It is quite hard to get an understanding of this signal from the time representation in the upper plot. However, the frequency representation in the lower plot gives a good grip of its nature: it is just the superposition of three sinusoids of different frequencies. This simple example illustrates the idea of why we use frequency representations. Basically, we try to get a simpler picture of some of the basic characteristics of the signal, which are usually not obvious from noisy and complex time representations.

The frequency representation of a signal is given by its Fourier Transform, which has innumerable applications in different scientific disciplines. In the specific case

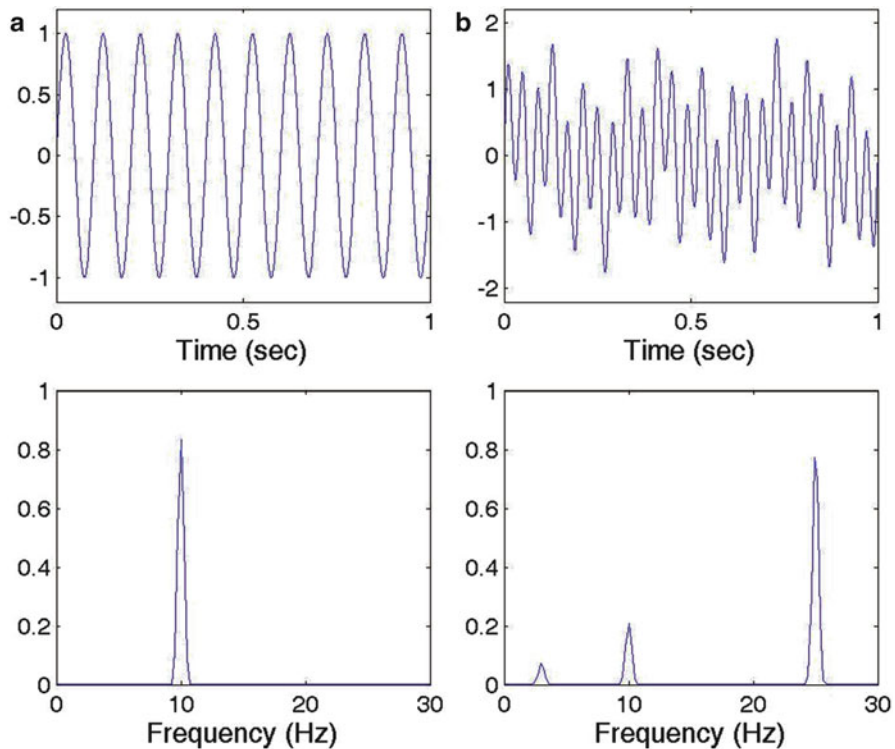


Fig. 2.1 (a) A sinusoidal signal in the time (*upper plot*) and frequency (*bottom plot*) domains. (b) A quasi-periodic signal. In this case, the Fourier Transform gives a simpler representation

of EEG signals, it is by far the most used quantitative tool, especially after the introduction of a very efficient and fast algorithm to calculate it, the Fast Fourier Transform (FFT; Cooley and Tukey 1965). In the next sections we will describe the basic ideas of the Fourier Transform and its implementation to the analysis of EEG signals together with some applications.

2.2 The Continuous Fourier Transform

There are four different types of Fourier Transforms, depending on whether the signal is continuous or discrete and on whether it is periodic or not. The derivations of these four transforms can be found in mathematical textbooks (see e.g., Oppenheim and Schaffer 1999). Here we focus on the general case of non-periodic signals, starting in this section with the continuous Fourier Transform and its basic properties.

The *continuous* Fourier Transform of a function $x(t)$ is defined as¹:

$$X(\omega) = \int_{-\infty}^{+\infty} x(t) e^{-j\omega t} dt \quad (2.1)$$

Where $e^{-j\omega t} = \cos \omega t - j \sin \omega t$ are complex exponentials and ω is the angular frequency related to the linear frequency f by $\omega = 2\pi \cdot f$. Equation 2.1 quantifies the amount of activity at each frequency ω of the original signal. The inverse Fourier Transform is defined as:

$$x(t) = \frac{1}{2\pi} \int_{-\infty}^{+\infty} X(\omega) e^{j\omega t} d\omega \quad (2.2)$$

and it gives back the original signal $x(t)$ expressed as a sum (or an integral to be precise) of sine and cosine functions of different frequencies, weighted by the Fourier coefficients $X(\omega)$. Note the symmetry of Eqs. 2.1 and 2.2, in the sense that one can exchange $x(t)$ by $X(\omega)$ just by changing the sign of the complex exponential and adding a normalization factor.

The Fourier Transform can be seen as the correlation between the signal $x(t)$ and the complex sinusoidal functions $e^{-j\omega t}$:

$$X(t) = \langle x(t), e^{-j\omega t} \rangle \quad (2.3)$$

This gives a very intuitive idea of the Fourier Transform. Indeed it is just the ‘matching’ between the original signal $x(t)$ and complex exponentials (or sine and cosine functions, if you prefer) of different frequencies.

2.3 The Discrete Fourier Transform

Digital signals have a finite length and are sampled with a certain sampling frequency. This finite length and sampling introduces several problems that we will discuss in this and the following sections.

Let us consider a discrete signal $x[n]$ $n = 1, \dots, N$, which has been derived from a continuous signal $x(t)$ by sampling at equal time intervals Δt (i.e. with a sampling frequency $f_s = \frac{1}{\Delta t}$). Obviously, the length of the signal is $T = N \cdot \Delta t$. Analogous to the continuous case (Eqs. 2.1 and 2.2), the *discrete* Fourier Transform is defined as:

$$X[k] = \sum_{n=0}^{N-1} x[n] e^{-j2\pi kn/N} \quad k = 0, \dots, N-1 \quad (2.4)$$

¹ To simplify convergences issues (see Mallat 1999; Strang and Nguyen 1997; Chui 1992 for details) let us just state that the Fourier transform exists for *absolutely integrable* functions; i.e. $\int |x(t)| dt < \infty$, or in mathematical notation $x(t) \in L^1(\mathbb{R})$. For discrete signals we require that $\sum |x[n]| < \infty$, which is always fulfilled by real signals since they have a finite length. We can recover the original signal using the inverse Fourier Transform (2.2) if $X(\omega) \in L^1(\mathbb{R})$.

and the signal $x[n]$ can be reconstructed with the inverse discrete Fourier Transform:

$$x[n] = \frac{1}{N} \sum_{k=0}^{N-1} X[k] e^{j2\pi kn/N} \quad (2.5)$$

The Fourier coefficients $X[k]$ are complex numbers that can be represented in Cartesian or polar forms, as:

$$X[k] = X_R[k] + jX_I[k] = |X[k]| e^{j\phi}, \quad (2.6)$$

where X_R and X_I denote the real and imaginary parts in the Cartesian representation, and $|X[k]|$ and ϕ denote the amplitude and phase in the polar representation. If we consider only real sequences $x[n]$, it can be easily shown that $X[k] = X^*[N-k]$ (where $*$ denotes complex conjugation). Then, the Fourier Transform gives a total of $N/2$ independent complex coefficients; that means N independent values. Since we can reconstruct a signal of N data points from the same number of independent Fourier values, the Fourier Transform is non-redundant.

From the time series $x[n]$ the discrete Fourier Transform gives the activity at frequencies f_k , with

$$f_k = \frac{k}{N\Delta t} \quad (2.7)$$

Clearly, the frequency resolution will be given by:

$$\Delta f = \frac{1}{N\Delta t} = \frac{1}{T} \quad (2.8)$$

According to the *Shannon Sampling Theorem* (Mallat 1999), the *Nyquist frequency* is defined as the highest frequency that can be resolved with a sampling period Δt :

$$f_N = \frac{1}{2\Delta t} = \frac{f_s}{2} \quad (2.9)$$

and it corresponds to $k = N/2$ in Eq. 2.7.

Note from Eq. 2.8 that we can increase the frequency resolution by increasing the signal length T . For a given signal length, decreasing the sampling period Δt does not change the frequency resolution, but the Nyquist frequency.

2.4 Aliasing

Let us illustrate the idea of aliasing with the example of Fig. 2.2. Suppose we sample a continuous sinusoidal signal with a relatively large sampling period Δt . Since our sampling is too sparse, we will not be able to resolve the underlying sinusoidal

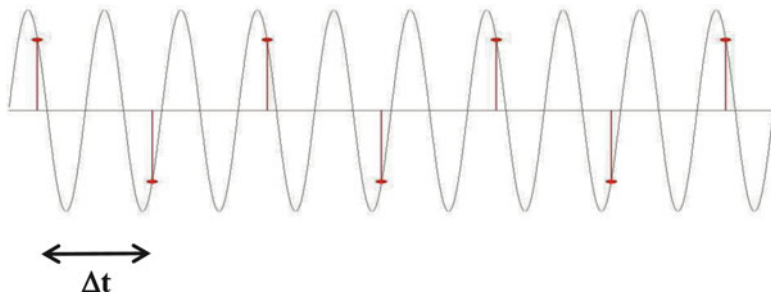


Fig. 2.2 Illustration of aliasing: An inadequate (*sparse*) sampling of the signal introduces spurious low frequency oscillations

signal and, even worse, we will see a slow oscillation that was not present in the original signal (just follow the markers of the digital samples). This effect is called aliasing: the introduction of spurious low frequencies due to an inadequate sampling of the signal.

Intuitively, to resolve a given oscillation we need at least two data points per period or in other words, the sampling frequency should be at least two times the frequency of the signal. This is just another way to state the Shannon Sampling Theorem and the Nyquist frequency of Eq. 2.9.

In real cases, such as for EEG recordings, we do not have a sinusoid of a given frequency for which we can set an appropriate sampling rate. Far from it, we have noisy signals with activity in different frequency bands and the sampling rate is set by our recording system. Then, in order to avoid aliasing, we have to guarantee that the Shannon Sampling Theorem is verified, namely, that the maximum frequency of the signal f_{\max} fulfills $f_{\max} < \frac{f_s}{2} = \frac{1}{2\Delta t}$. This is achieved by using low pass ‘anti-aliasing’ filters. It has to be remarked that anti-aliasing filtering has to be performed by hardware before the digitization of the signal. Once the signal has been digitized, there is no way to get rid of aliasing!

2.5 Fast Fourier Transform

The calculation of the discrete Fourier Transform with Eq. 2.4 requires N^2 complex multiplications, because for each of the N discrete frequencies k we have to calculate a sum of N multiplications with complex exponentials. This may take too long for large N but, fortunately, it is possible to reduce dramatically the computation speed by using the Fast Fourier Transform algorithm (FFT; Cooley and Tukey 1965). The introduction of the FFT has revolutionized the analysis of digital signals and, in particular, it boosted the study of EEGs in the frequency domain. A detailed description of the FFT algorithm is outside the scope of this book and can be found in most signal processing textbooks (see e.g., Oppenheim and Schaffer 1999).

The basic idea is to avoid redundancies given that in Eq. 2.4 we end up calculating the same multiplications several times. In particular, the complex exponential of Eq. 2.4 is periodic and the permutation of n and k give the same result. So, it is possible to reduce the number of calculations to be done. If N is a power of 2 (e.g., 64, 128, 256, ...), it can be shown that the original N -point discrete Fourier Transform can be expressed in terms of two $N/2$ -point transforms. Since the computing time goes as $O(N^2)$ this results in a faster processing time. Even better, each of the two $N/2$ -point transforms can also be expressed in terms of $N/4$ -point transforms and so on until we are left with 2-point sequences. It can then be shown that the computing time in this case is of the order $N \log_2 N$, which is clearly faster than N^2 . The difference in processing time becomes critical for large datasets. For example, for 64 data points the FFT is about ten times faster than the direct calculation of Eq. 2.4, and for a million data points (just about half an hour recording of one channel with a sampling frequency of 500 Hz) the FFT is over 50,000 times faster!

2.6 Power Spectrum

From the complex Fourier coefficients $X[k]$ of Eq. 2.4 we can define the *periodogram* as:

$$I_{xx}[k] = |X[k]|^2 = X[k] \cdot X^*[k] \quad (2.10)$$

Considering that the signal is a stationary stochastic process, the periodogram is a raw estimation of the *power spectral density* of the signal (the power spectrum).

In Sect. 2.3 we stressed that the Fourier Transform is non-redundant. This means that if we have a real signal with N data points, the Fourier Transform gives N independent values (or $N/2$ complex coefficients) from which we can get back the original signal. No information is gained or lost. This is true both for linear and nonlinear signals. However, it is well known that the Fourier Transform is only suited for linear signals and cannot characterize nonlinear patterns. How can this be?

Recall Eq. 2.6 where we showed that the Fourier coefficients can be written in polar form in terms of an amplitude and a phase. A stationary nonlinear signal, say a sequence of epileptic spikes, is represented in the Fourier domain as a sum of sinusoids, each of them added with a particular phase to reproduce the nonlinear spike shapes. But if we disregard the phases, we lose critical information that characterizes the nonlinear pattern of the original signal (i.e. the spikes). Now look again at Eq. 2.10. It is just the square of the amplitude of the Fourier coefficients defined in Eq. 2.6. The problem is that we usually look only at the power spectrum of the signal and we disregard the phase. This is the reason why we lose information about nonlinear structures with the Fourier Transform. But even if we keep the phase information, the representation of nonlinear patterns as sums of sinusoids at particular phases seems quite cumbersome. In practice, we use the Fourier Transform to extract the linear characteristics of the signals and we turn to other methods to study nonlinear processes.

2.7 Leakage and Windowing

We mentioned that the periodogram is a raw estimate of the power spectrum. Let us illustrate this with the example of Fig. 2.3. The sinusoid on the left has an exact number of cycles in the 0.5 s period of the signal and its periodogram gives a single peak at 6 Hz. The sinusoid on the right, on the other hand, has a non-integer number of cycles in the period considered and its periodogram gives an activity that is spread between 2 and 8 Hz. This smearing of the power spectrum estimation is called leakage.

To understand where leakage comes from we first need to realize that every real signal has a limited duration and that when we calculate the discrete Fourier Transform we make the implicit assumption that the signal repeats itself periodically outside the time range in which it has been recorded. It will take us too long to demonstrate this, but the basic idea is that discretizing the signal (as we do by sampling it) imposes that the Fourier Transform will be periodic, and discretizing

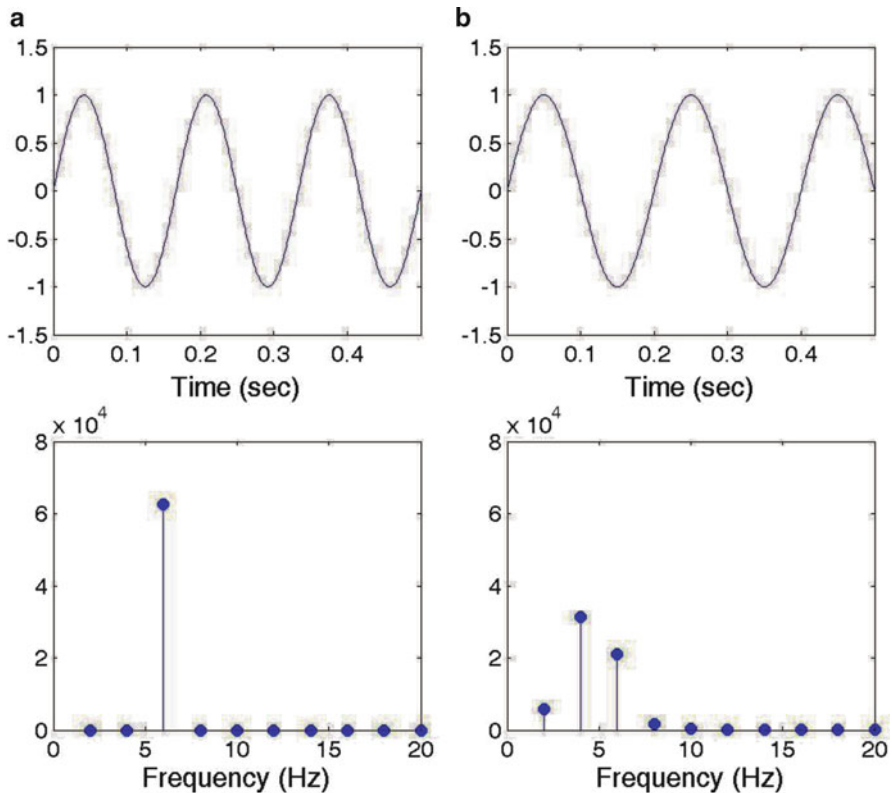


Fig. 2.3 Example of leakage. The sinusoid in (a) has an integer number of cycles and its power spectrum gives a single peak at 6 Hz. The sinusoid in (b) has a non-integer number of cycles and its power spectrum is smeared around 5 Hz

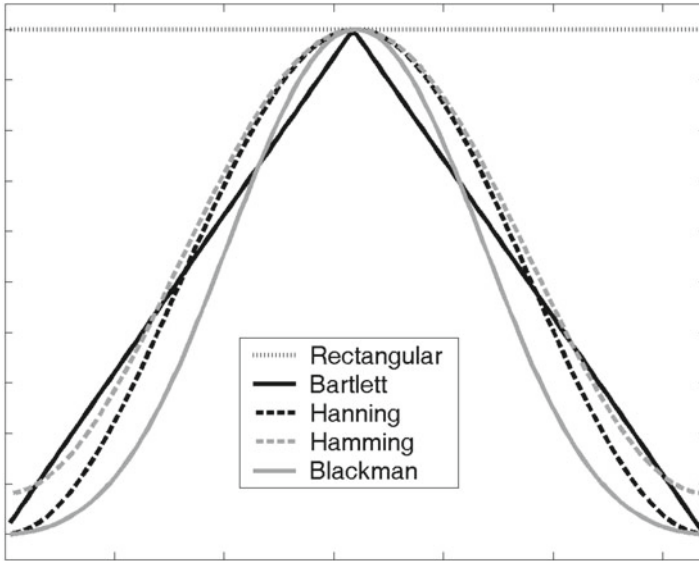


Fig. 2.4 Taper windows used to diminish leakage effects

the frequencies (as we also have to do, since we cannot get a continuous distribution of frequencies for real data) imposes periodicity in the time domain (Oppenheim and Schaffer 1999). If we repeat the signal in Fig. 2.3a over and over again, we will have a smooth sinusoid, since the starting point is exactly the continuation of the final one. On the contrary, if we repeat the signal on Fig. 2.3b we will be introducing discontinuities. These discontinuities are the ones causing leakage. In other words, if we want to synthesize the signal in Fig. 2.3b, including the discontinuities caused by repetition, we will have to use in principle all the components of the spectrum and especially those between 2 and 8 Hz.

A simple way to avoid this would be to take an integer number of cycles. However, real signals have activity at different frequencies and it is in general not possible to define a single periodicity. An alternative approach to avoid these discontinuities is by tapering the borders of the signal using an appropriate window function. This procedure is known as *windowing*. There is, however, a tradeoff when windowing because on the one hand, it diminishes leakage effects but on the other hand it also decreases the frequency resolution. A precise mathematical formulation is outside the scope of this book (see Oppenheim and Schaffer 1999; Jenkins and Watts 1968), but intuitively we can see that a strong tapering decreases the ‘effective’ length of the signal in which the different frequencies are defined and, as shown in Eq. 2.8, the length of the signal determines its frequency resolution. Several windows have been proposed to optimize this tradeoff and their advantages and disadvantages depend on the application. Among these, the most popular windows are the Bartlett, Hanning, Hamming and Blackman, as shown in Fig. 2.4. For a comprehensive review of the properties of these windows we refer to Oppenheim and Schaffer (1999) and Jenkins and Watts (1968).

2.8 Variance of the Power Spectrum: Periodogram Averaging

It can be shown that, besides the problem of leakage, the periodogram is not a statistically consistent estimate of the power spectrum because its variance does not approach zero with increasing data length (Oppenheim and Schaffer 1999; Dumermuth and Molinari 1987). Furthermore, for large data sets the periodogram tends to vary rapidly with frequency. These variations arise from the estimation process per se and result in a ‘random looking’ power spectrum. To get a smoother estimate, Bartlett proposed to average several periodograms (Bartlett 1953). This can be done by dividing the dataset into a number of segments, calculating the periodogram for each segment and then averaging the periodograms. This method was further developed by Welch who showed that better estimates are obtained by using half-overlapping windows (Welch 1967). Periodogram averaging, known as the Bartlett or Welch method, makes the power spectrum smoother and reduces its variability (which now tends to zero for large data). It can also be shown (Oppenheim and Schaffer 1999) that this averaging procedure is equivalent to a smoothing of the original periodogram with a spectral window. Another advantage is that, due to the averaging that is involved, it is possible to estimate error bars and confidence intervals.

Periodogram averaging copes with the problem of variability of the power spectrum estimation but, as usual, there is no free lunch! Again we face a tradeoff. On the one hand, the more segments we use for averaging the smaller the variability and the smoother the power spectrum will look. But on the other hand, the more segments we use, the less number of data points per segment and, consequently, the lower the spectral resolution (see Eq. 2.8).

2.9 Practical Remarks for Estimating the Power Spectrum of EEG Signals

From the discussions of the previous sections we may conclude that the design of an optimal frequency analysis of EEG signals is more a sort of art than a standardized procedure. Indeed there are many tradeoffs and limitations we should be aware of. Having said this, there are many common situations we face over and over again when doing a frequency analysis of EEG signals. Therefore, we can set some general guidelines for its implementation. Let us deal with each problem one at a time:

- *Sampling rate:* It should be at least two times the maximum frequency of interest in the EEG signal. In our days it is relatively common (and not expensive) to have recording systems with sampling frequencies of 500 Hz or higher. With 500 Hz it is possible to study frequencies of up to 250 Hz, which should be enough for most applications.²

²For cases like the study of fast propagating seizures, the analysis of early evoked potentials, or the analysis of fast ripples, a sampling of 1,000 Hz is the minimum admissible given that it is crucial to have a resolution of the order of a millisecond or less.

- *Aliasing*: Ideally it should be dealt with by the acquisition system with a low-pass ‘anti-aliasing’ filter set in the hardware. If this is not possible, the signal should be oversampled when recording (e.g., with 1,000 Hz), then low pass filtered and decimated.
- *Power spectrum estimation*: In order to reduce the variability of the power spectrum and wash out a ‘noisy-looking’ appearance, we can use the periodogram averaging method described in Sect. 2.8. This approach also helps to cope with other problems such as stationarity and artifacts as we will see in the next points. The number of segments to be used is determined by the length of the dataset and it should be in principle more than 10 (ideally 30 or more, depending on the application).
- *Segment length*: The length of the segments used for the average periodogram determines the frequency resolution. The larger the segments the better the frequency resolution. However, we want to use segments that are not too long, so they do not include artifacts, and the signal can be considered stationary to a first approximation. In practice, segments of 2 s seems appropriate, thus giving a frequency resolution of 0.5 Hz (see Eq. 2.8). Due to details of the implementation of the Fast Fourier Transform algorithm, to increase computational speed it is also desirable that the length of the segments is a power of 2 (e.g., 64, 128, 256, etc.). In search for spatial images of amplitude and phase in the EEG and ECoG (part II of this book) the optimal window duration may be reduced to the range of 0.1 s, which gives poor frequency resolution but excellent temporal resolution for the calculation of the amplitude and phase. The coarse graining of frequency turns out to be an advantage, because it facilitates tracking of EEG and ECoG images with frequency modulation (FM).
- *Leakage*: To diminish leakage we can taper each of the segments used for periodogram averaging with e.g., a Hanning window.
- *Stationarity*: One of the main assumptions we make to estimate the power spectrum of EEGs is that they can be treated as stationary stochastic signals. If they are not stationary, then the spectrum may be meaningless (see Figure 3.1). For periodogram averaging we must then assume that all segments correspond to the same stochastic process. This can be actually checked by observing the variability of the periodograms and any particular trend. An obvious pitfall would be to include segments corresponding to different brain states, such as mixing periods of normal and epileptic EEG activity or periods of awake and sleep EEG. Furthermore, we should also check that the signal can be considered stationary within each segment, which imposes a limitation to the segment length.
- *Artifacts*: Due to its large amplitude, artifacts can seriously contaminate the power spectrum. For estimating the power spectrum using the Welch method (i.e. averaging the periodograms of different segments of the signal), it is therefore advisable to select segments that are artifact free. Artifacts can be checked either visually or with advanced artifact detection methods, such as Independent Component Analysis (Jung et al. 2000).

2.10 Applications of EEG Frequency Analysis

2.10.1 EEG Frequency Bands

In the first report of human EEG recordings, Hans Berger already noted the presence of different brain oscillations (Berger 1929). In particular, he reported rhythmic activity of around ten cycles per second, most pronounced in the occipital electrodes with eyes closed. These oscillations, which he named *alpha rhythms*, were dramatically decreased by the influx of light with eyes opening. This effect is what in our days we call *alpha blocking* and it is one of the most dramatic and simplest demonstrations of how the EEG reflects brain processes. We define *reactivity* as the ratio of alpha activity with eyes closed and eyes open. The degree of reactivity varies from subject to subject, but it is generally accepted that a lack of reactivity is an abnormal finding (Niedermeyer 1993). Berger also described oscillatory activity of higher frequencies, which he called the *beta rhythms*. They appeared with eyes open and to some degree also with eyes closed when the subjects performed mental calculations. Following Berger's seminal work, different EEG oscillations and their correlation to different brain states, functions and pathologies had been thoroughly studied, especially after the introduction of digital recordings and the Fast Fourier Transform (Cooley and Tukey 1965). Based mainly on their function and localization, EEG oscillations have been grouped into frequency bands. Here we just give a brief summary of them and we refer to the excellent review of Niedermeyer (1993) for more details.

Figure 2.5 shows an EEG recording of 20 s and its corresponding power spectrum. The vertical lines mark the limits of the standard EEG frequency bands:

- Alpha rhythms (7.5–12.5 Hz): they appear spontaneously in normal adults during wakefulness, under relaxation and mental inactivity conditions. They are best seen with eyes closed, most pronounced in the occipital locations.
- Beta rhythms (12.5–30 Hz): they are best defined in central and frontal locations, with less amplitude than alpha waves. They are enhanced upon mental calculations, expectancy or tension over the entire surface of the scalp (Fig. 2.6 and Fig. 10.9).
- Theta rhythms (3.5–7.5 Hz): They are typical during deep sleep. They play an important role in infancy and childhood. In the awake adult, high theta activity is considered abnormal and related to brain disorders, such as epilepsy.
- Delta rhythms (0.5–3.5 Hz): They are also characteristic of deep sleep stages. Depending on their morphology, localization and rhythmicity, delta oscillations can be normal as in slow wave sleep or pathological as in brain tumors.
- Low Gamma rhythms (30–60 Hz in human EEG, 30–80 Hz in animal ECoG): Of minor interest until the 1990s, gamma oscillations became very popular after they have been proposed to play a major role in linking stimulus features into a single perception (binding theory; Gray et al. 1989). Although the validity of the

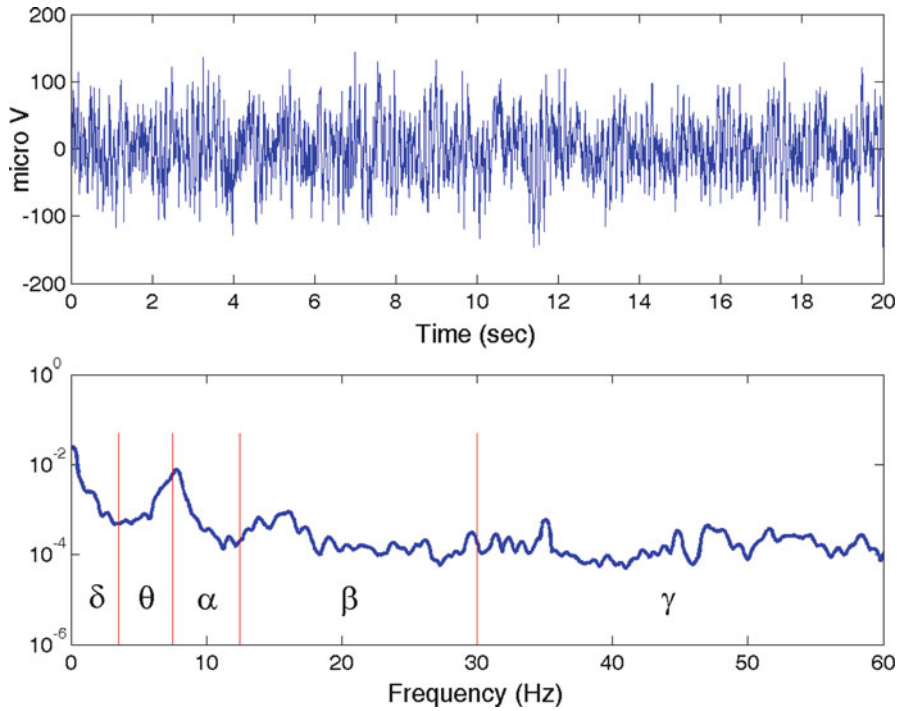


Fig. 2.5 EEG frequency bands

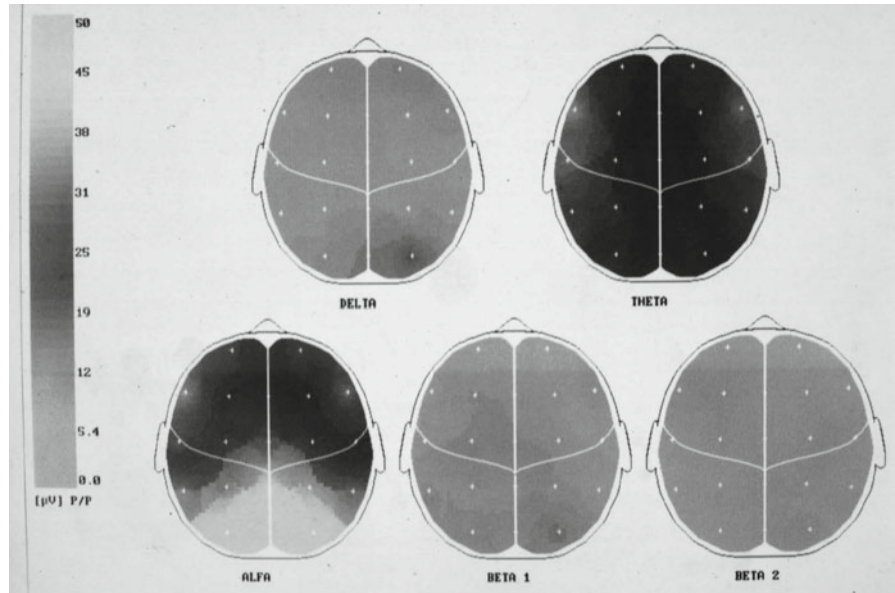


Fig. 2.6 Topographical mapping of the different EEG frequency bands from a normal EEG recording taken with eyes closed

binding theory is still under dispute, several follow up works have shown correlations of gamma activity with different sensory and cognitive processes, notably during visual, auditory, somatic and olfactory perception (see Chaps. 8 and 9) as well as with attention.

- High gamma rhythms (variously defined between 80–120+) also called epsilon rhythms have been found in human and animal ECoG in association with chattering action potentials (Ray and Maunsell 2011)

It should be emphasized that not all EEG oscillations of the same frequency have the same function. For example, delta oscillations are normal during slow wave sleep but are a clear sign of abnormality in awake states, given that 3 Hz spike and wave discharges are a characteristic sign of absence seizures. Mu rhythms have a frequency similar to that of the occipital alpha rhythm, but they are observed in central locations and are related to motor functions. Spindle oscillations have also a periodicity of about 10 Hz, but they are characteristic of sleep stage 2.

Since EEG patterns are quite variable and complex, visual inspection is still one of the preferred ways to analyze EEG recordings by expert electroencephalographers. This is more an art than an exact science and it requires years of training. Clearly, visual inspection is very subjective and a quantitative approach should in principle be preferred. However, it must be said that some training in EEG visual inspection is particularly useful before embarking in automatic and quantitative EEG analysis, at least to have a feeling of what type of patterns and characteristics of the raw EEG we are trying to quantify. Most of quantitative electroencephalography deals with the analysis of the EEG frequency bands described above. Several parameters have been defined to quantify them, such as the relative power between bands (being the most used the alpha/theta ratio), reactivity (ratio between eyes closed/eyes open alpha activity), asymmetry index (the difference between the left and right power), etc. (Nuwer et al. 1994). Moreover, statistical techniques can be used in order to establish normal ranges and their deviations with several pathologies (John et al. 1987).

2.10.2 Topographic Analysis

The information from the different electrodes can be arranged in topographic maps (Gotman 1990; Gevins 1987; Lehmann 1987; Lopes da Silva 1993a). These algorithms usually use linear or quadratic interpolations between the 3 or 4 nearest recording sites. One critical point is the election of the reference, since the use of single electrode references can distort the maps near the reference site (Lehmann 1971, 1987) (see Fig. 10.9). Several suggestions were proposed in order to avoid this distortion, among them the use of averaged references and the use of the average of the derivatives of the EEG signals (Lehmann 1987; Lopes da Silva 1993b). Another important issue to be considered is how to project a three dimensional head into a two dimensional map.

The use of topographic plots started more than 30 years ago (Walter et al. 1966; Lehmann 1971), but it was after the introduction of color topographic maps by Duffy et al. (1979) that they became widely accepted and started to be used in several medical centers. With these plots it is easy to visualize asymmetries and to localize the activity of the different frequency bands. Furthermore, the topographic maps complement the quantitative parameters described in the previous sections for the characterization of normal EEG patterns and the study and diagnosis of several pathologies (Duffy 1986; Maurer and Dierks 1991; Pfurtscheller and Lopes da Silva 1988).

Figure 2.6 shows the topographic map of the EEG recording of a normal subject with eyes closed. Five different frequency bands are plotted. As expected, the power is homogeneously distributed in all the frequency bands, except in alpha, where there is a symmetrical increase in the posterior locations. This increase reflects the presence of the normal spontaneous alpha activity described above.

Before leaving this section we stress that topographic maps give a static picture of the brain activity. Later we will describe a radically different approach to study how EEG activity propagates not only in time but also in space. These are the EEG images of the title of our book. In our chapters we will demonstrate the methods by which we succeed in extracting finely textured patterns of amplitude from the blandly uniform distributions of potential shown in Fig. 2.6 (see Sect. 10.5). The textured images are formed by amplitude and phase modulation (AM and PM) of spatially coherent carrier waves in the beta range. They recur at rates in the theta range as brief epochs that resemble cinematic frames. They contain cognitive information, because they are classifiable with respect to sensory stimuli that human subjects are perceiving as the patterns fly past. Part II of this book is directed to describe how to find these patterns, explain how they are generated, and interpret what they contribute to our understanding of human cognitive neurodynamics.

2.11 Summary

In this chapter we reviewed the basic background of the Fourier Transform and its use in the analysis of EEG signals. One important application is the comparison between the power at different frequency bands and their topological distribution. Normative values have been established and large deviations from them can reflect pathological cases. Moreover, deviations from background values in subjects who are engaged in cognitive tasks may direct us to discover EEG and ECoG correlates of cognition. This analysis is already adapted to many commercial systems and it is used in several medical centers. Although quantitative parameters are very useful and can be easily extracted from the EEG in an automated way, the visual inspection of the recordings should not be left aside, in order to avoid misinterpretations due to non-stationarity, artifacts, etc. In fact, topographic mapping and quantitative values should be considered as a complement and not as a replacement of visual inspection of the EEG.

The frequency analysis allowed by the Fourier Transform has been by far the most useful quantification of EEG activity. It has, however, three main limitations:

1. The Fourier Transform requires stationarity of the signal. For the purpose of estimating the power spectrum, the EEGs can be regarded as quasi-stationary only on the order of a few seconds (Blanco et al. 1995). Obviously, the Fourier Transform is also not well suited for the analysis of transient responses as in the case of Evoked potentials.
2. The Fourier Transform is very accurate at characterizing the frequency composition of a signal, but it gives no time information. In other words, we can very well define the activity at a particular frequency but we can not tell when exactly this frequency occurs and how it evolves in time. This is of course related to the issue of stationarity. It justifies the use of time varying methods, like the short-time Fourier Transform, Wavelets or the Hilbert transform to be described in the next chapters.
3. The Fourier Transform is not optimal to characterize non-linear signals. As we described in Sect. 2.6, non-linear patterns, for example epileptic spikes, are represented in the Fourier domain as complex combinations of different frequencies with precise phase relationships. Since we usually only look at the power spectrum and disregard the phase information, the non-linear nature of the signal is lost. But even if we decide to keep the phases, describing a spike as a sum of sinusoids with a certain phase relationship is very cumbersome and other methods such as wavelets (see Chap. 4) may be preferred.

References

- Bartlett MS (1953) An introduction to stochastic processes with special reference to methods and applications. Cambridge University Press, Cambridge, MA
- Berger H (1929) Über das Elektroencephalogramm des Menschen. *Arch Psychiat Nervenkr* 87:527–570
- Blanco S, Garc a H, Qui an Quiroga R, Romanelli L, Rosso OA (1995) Stationarity of the EEG series. *IEEE Eng Med Biol* 14:395–399
- Cooley WJ, Tukey JW (1965) An algorithm for the machine calculation of complex Fourier series. *Math Comput* 19:297–301
- Duffy FH, Burchfiel JL, Lombroso CT (1979) Brain electrical activity mapping (BEAM): a method for extending the clinical utility of EEG and evoked potential data. *Ann Neurol* 5:309–321
- Duffy FH (1986) Topographic mapping of brain electrical activity. Butterworths, London
- Dumermuth G, Molinari L (1987) Spectral analysis of EEG background activity. In: Gevins A, R mond A (eds) *Handbook of electroencephalography and clinical neurophysiology, Vol. I: Methods of analysis of brain electrical and magnetic signals*. Elsevier, Amsterdam, pp 85–130
- Gevins AS (1987) Overview of computer analysis. In: Gevins A, R mond A (eds) *Handbook of electroencephalography and clinical neurophysiology, Vol. I: Methods of analysis of brain electrical and magnetic signals*. Elsevier, Amsterdam, pp 31–83
- Gotman J (1990) The use of computers in analysis and display of EEG and evoked potentials. In: Daly DD, Pedley TA (eds) *Current practice of clinical electroencephalography*, 2nd edn. Raven Press, New York, pp 51–83

- Gray C, König P, Engel A, Singer W (1989) Oscillatory responses in cat visual cortex exhibit inter-columnar synchronization which reflects global stimulus properties. *Nature* 338:335–337
- Jenkins GM, Watts DG (1968) Spectral analysis and its applications. Holden-Day, San Francisco
- John ER, Harmony T, Valdes-Sosa P (1987) The use of statistics in electrophysiology. In: Gevins A, Rémond A (eds) *Handbook of electroencephalography and clinical neurophysiology*, Vol. I: Methods of analysis of brain electrical and magnetic signals. Elsevier, Amsterdam, pp 497–540
- Lehmann D (1971) Multichannel topography of human alpha EEG fields. *Electroencephalogr Clin Neurophysiol* 31:439–449
- Lehmann D (1987) Principles of spatial analysis. In: Gevins A, Rémond A (eds) *Handbook of electroencephalography and clinical neurophysiology*, Vol. I: Methods of analysis of brain electrical and magnetic signals. Elsevier, Amsterdam, pp 309–354
- Lopes da Silva FH (1993a) EEG analysis: theory and practice. In: Niedermeyer E, Lopes da Silva FH (eds) *Electroencephalography: basic principles, clinical applications and related fields*, 3rd edn. Williams and Wilkins, Baltimore, pp 1097–1123
- Lopes da Silva FH (1993b) Computer-assisted EEG diagnosis: pattern recognition and brain mapping. In: Niedermeyer E, Lopes da Silva FH (eds) *Electroencephalography: basic principles, clinical applications and related fields*, 3rd edn. Williams and Wilkins, Baltimore, pp 1063–1086
- Jung T-P, Makeig S, Humphries C, Lee TW, McKeown MJ, Iragui V, Sejnowski TJ (2000) Removing electroencephalographic artifacts by blind source separation. *Psychophysiology* 37:163–78
- Maurer K, Dierks T (1991) *Atlas of brain mapping*. Springer, Berlin
- Niedermeyer E (1993) The normal EEG of the waking adult. In: Niedermeyer E, Lopes da Silva FH (eds) *Electroencephalography: basic principles, clinical applications and related fields*, 3rd edn. Williams and Wilkins, Baltimore, pp 131–152
- Nuwer MR, Lehmann D, Lopes da Silva FH, Matsuoka S, Sutherling W, Vivert JF (1994) IFCN guidelines for topographic and frequency analysis of EEGs and EPs. Report of and IFCN committee. *Electroencephalogr Clin Neurophysiol* 91:1–5
- Oppenheim A, Schaffer R (1999) *Discrete-time signal processing*. Prentice Hall, London
- Pfurtscheller G, Lopes da Silva FH (eds) (1988) *Functional brain imaging*. Huber, Toronto
- Ray S, Maunsell JHR (2011) Different origins of gamma rhythm and high-gamma activity in macaque visual cortex. *PLoS Biol* 9:e1000610
- Walter D, Rhodes J, Brown D, Adey W (1966) Comprehensive spectral analysis of human EEG generators in posterior cerebral regions. *Electroencephalogr Clin Neurophysiol* 20:224–237
- Welch PD (1967) The use of Fast Fourier Transform for the estimation of power spectra: a method based on time-averaging over short modified periodograms. *IEEE Trans Audio-Electroacoust* 15:70–73

Imaging Brain Function With EEG
Advanced Temporal and Spatial Analysis of
Electroencephalographic Signals

Freeman, W.; Quiroga, R.Q.

2013, XXII, 250 p., Hardcover

ISBN: 978-1-4614-4983-6